BBA - Molecular and Cell Biology of Lipids 1865 (2020) 158634

Contents lists available at ScienceDirect

BBA - Molecular and Cell Biology of Lipids

journal homepage: www.elsevier.com/locate/bbalip

Lipidomic characterization of exosomes isolated from human plasma using various mass spectrometry techniques

Ondřej Peterka[a], Robert Jirásko[a], Michaela Chocholoušková[a], Ladislav Kuchař[b], Denise Wolrab[a], Roman Hájek[a], David Vrána[c], Ondřej Strouhal[c], Bohuslav Melichar[c], Michal Holčapek[a,*]

[a] University of Pardubice, Faculty of Chemical Technology, Department of Analytical Chemistry, Studentská 573, 532 10 Pardubice, Czech Republic
[b] Research Unit for Rare Diseases, Department of Pediatrics and Adolescent Medicine, First Faculty of Medicine, Charles University and General University Hospital in Prague, Prague, 12808, Czech Republic
[c] Department of Oncology, Faculty of Medicine and Dentistry, Palacký University and University Hospital, I.P. Pavlova 6, 775 20 Olomouc, Czech Republic

ARTICLE INFO

Keywords:
Lipidomics
Lipids
Exosomes
Plasma
Mass spectrometry
Supercritical fluid chromatography
Liquid chromatography

ABSTRACT

Ultrahigh-performance supercritical fluid chromatography - mass spectrometry (UHPSFC/MS), ultrahigh-performance liquid chromatography - mass spectrometry (UHPLC/MS), and matrix-assisted laser desorption/ionization (MALDI) - MS techniques were used for the lipidomic characterization of exosomes isolated from human plasma. The high-throughput methods UHPSFC/MS and UHPLC/MS using a silica-based column containing sub-2 μm particles enabled the lipid class separation and the quantitation based on exogenous class internal standards in < 7 minute run time. MALDI provided the complementary information on anionic lipid classes, such as sulfatides. The nontargeted analysis of 12 healthy volunteers was performed, and absolute molar concentration of 244 lipids in exosomes and 191 lipids in plasma belonging to 10 lipid classes were quantified. The statistical evaluation of data included principal component analysis, orthogonal partial least square discriminant analysis, S-plots, p-values, T-values, fold changes, false discovery rate, box plots, and correlation plots, which resulted in the information on lipid changes in exosomes in comparison to plasma. The major changes were detected in the composition of triacylglycerols, diacylglycerols, phosphatidylcholines, and lysophosphatidylcholines, whereby sphingomyelins, phosphatidylinositols, and sulfatides showed rather similar profiles in both biological matrices.

1. Introduction

The maintenance of homeostasis on the level from cells to whole organism requires a complex cell-signaling network. Information exchange mechanisms involve not only local cell-to-cell contact interactions, but also the transfer of signaling molecules over longer distance by microvesicles and exosomes. Microvesicles and exosomes are particles that may be differentiated by the physicochemical properties and origin [1–3]. The microvesicles represent larger vesicles generated by budding plasmatic membrane, and consequently their composition is closer to plasma membrane. In contrast, exosomes are related to the endocytosis followed by the maturation of early endosomes to multivesicular bodies (MVB) with intraluminal vesicles later released from the cell as exosomes by the fusion of MVB with plasma membrane. This process points to different composition of exosomes, which are composed from the intracellular material encapsulated by the endosomal membrane (Fig. 1) [1,2].

The biological function of microvesicles and exosomes is the long distance cell to cell communication, transportation of enzymes, disposal of superfluous cellular content and the stimulation or inhibition of the immune response [4]. The production and composition of exosomes can be different in cancer and various types of exosomes have been used as potential lipidomic biomarkers for screening of prostate cancer [5,6], colorectal cancer [7], lung cancer [8], or breast cancer [8,9].

Exosomes are nano-particles (30–100 nm) that are composed mainly of DNA, RNA, lipids, and proteins [4,10,11]. Exosomes can be isolated from biological fluids including urine [6,12], plasma [13], saliva [14], and breast milk [4], or from cells [5,7,8,15]. Several methods are being used for the isolation of total exosomes, such as centrifugation [4,10,11], chromatography [4,10,11,13], filtration [4,10,11], and precipitation [4,10]. Different approaches for exosomal isolation are necessary for the separation of their specific subpopulations in contrast to the isolation of total exosomes [2,16]. The yield and purity of exosomes differ according to the method used and the type of biological matrix [4,10,11]. Exosomes can be characterized by several methods, e.g., flow cytometry [4,11,17,18], Western blot [17,18], transmission electron microscopy

* Corresponding author.
E-mail address: Michal.Holcapek@upce.cz (M. Holčapek).

https://doi.org/10.1016/j.bbalip.2020.158634
Received 19 October 2019; Received in revised form 30 December 2019; Accepted 17 January 2020
Available online 21 January 2020
1388-1981/

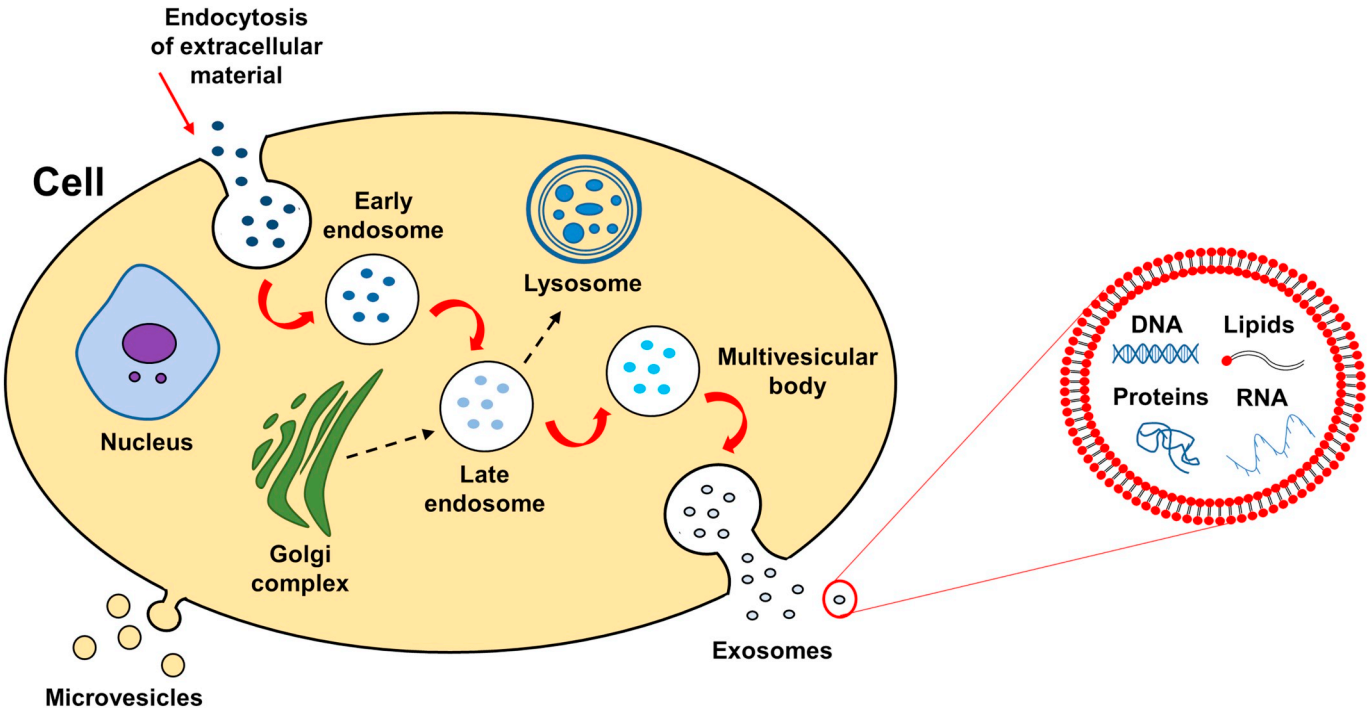

Fig. 1. Scheme of cell processes leading to the formation and release of microvesicles and exosomes, which mainly consist of DNA, RNA, proteins, and lipids.

[4,17], and fluorescence microscopy [4].

Lipidomics is a subgroup of metabolomics aiming at the analysis of lipid species. Lipids play important roles in cells and have various biological functions, such as energy storage or serving as precursors for metabolic processes. The dysregulation of lipid metabolism in cancer [19,20], neurodegenerative diseases [19–21], and cardiovascular diseases [22] has been reported in the literature. Individual lipids differ in the length of nonpolar fatty acyl chain(s) and polar/ionic head groups. The LIPID MAPS classification and nomenclature are widely used in the lipidomic studies [23].

Mass spectrometry (MS) is currently the principal technique for the lipid analysis. There are two fundamental approaches, direct infusion or chromatography coupled to MS. UHPLC is the most widely used chromatographic technique for the lipidomic separation [19]. Reversed-phase chromatography allows a separation according to their fatty acyl composition into individual species, which causes the elution of the internal standard (IS) at different times. Normal-phase and hydrophilic interaction liquid chromatography (HILIC) are used for the class separation. High-separation efficiency and short analysis time are achieved by UHPSFC and UHPLC using columns packed with sub-2 μm particles or by core-shell particle columns. UHPSFC enables the separation of non-polar and polar lipids together in one run [24–26]. MALDI coupled to Orbitrap mass spectrometry uses high mass resolution and tandem mass spectra for the identification [27]. Previous works showed the comparison of lipidomic quantitation by various MS based approach [24,28] with conclusions that lipidomic profiles determined by different methods for the same samples are comparable, but not completely identical, and some discrepancies cannot be considered as negligible. The recent work suggested the use of data normalization in relation to one reference sample (e.g., NIST SRM 1950) determined by all compared approaches, which improves significantly the quality of mutual comparison.

The aim of this work is the comparison of the lipidomic composition of exosomes isolated from human plasma of 12 healthy volunteers and plasma of the same volunteers using three MS approaches to identify major differences between these two biological materials. Absolute concentrations of lipid species were determined, and relative data were used for better visualization of changes inside the individual classes. Statistical tools and projection methods were applied to investigate differences between both biological materials.

2. Experimental

2.1. Materials

Acetonitrile, 2-propanol, methanol (all HPLC/MS grade), hexane, chloroform stabilized with 0.5–1% ethanol (both HPLC grade), ammonium acetate, and 9-aminoacridine were purchased from Sigma-Aldrich (St. Louis, MO, USA). Deionized water was prepared with a Milli-Q Reference Water Purification System (Molsheim, France). Carbon dioxide grade (99.995%) was purchased from Messer Group Gmbh (Bad Soden, Germany). Internal standards triacylglycerol (TG) 19:1/19:1/19:1, diacylglycerol (DG) 12:1/0:0/12:1, and monoacylglycerol (MG) 19:1/0:0/0:0 were purchased from NuChek (Elysian, MN, USA). D7-cholesteryl ester (D7-CE) 16:0, D7-cholesterol (D7-Chol) 27:1, D7-phosphatidylinositol (D7-PI) 18:1/15:0, lysophosphatidylcholine (LPC) 17:0/0:0, lysophosphatidylethanolamine (LPE) 14:0/0:0, phosphatidylcholine (PC) 14:0/14:0, phosphatidylethanolamine (PE) 14:0/14:0, phosphatidylglycerol (PG) 14:0/14:0, phosphatidylserine (PS) 14:0/14:0, ceramide (Cer) 18:1/12:0, sphingomyelin (SM) 18:1/12:0, sulfatide (SHexCer) 18:1/12:0 were purchased from Avanti Polar Lipids (Alabaster, AL, USA). The internal standard mixture (IS Mix) for each quantified lipid class was prepared by mixing of all IS at appropriate concentrations. Final concentrations for exosomes and plasma are shown in Table S-1. Stock solutions and IS Mix were diluted in a chloroform – 2-propanol mixture (1:4, v/v).

Plasma of healthy male volunteers was obtained at the Department of Oncology, Faculty of Medicine and Dentistry, Palacký University and University Hospital Olomouc, Czech Republic. The blood collection was performed after overnight fasting with the recommendation to avoid heavy meals and alcohol consumption in the evening before the blood collection. The study was approved by the institutional ethical committee agreement, and all subjects signed informed consent. Samples were stored at −80 °C, then transported from the hospital to the analytical laboratory at −20 °C on dry ice, and then stored again at −80 °C until the sample preparation.

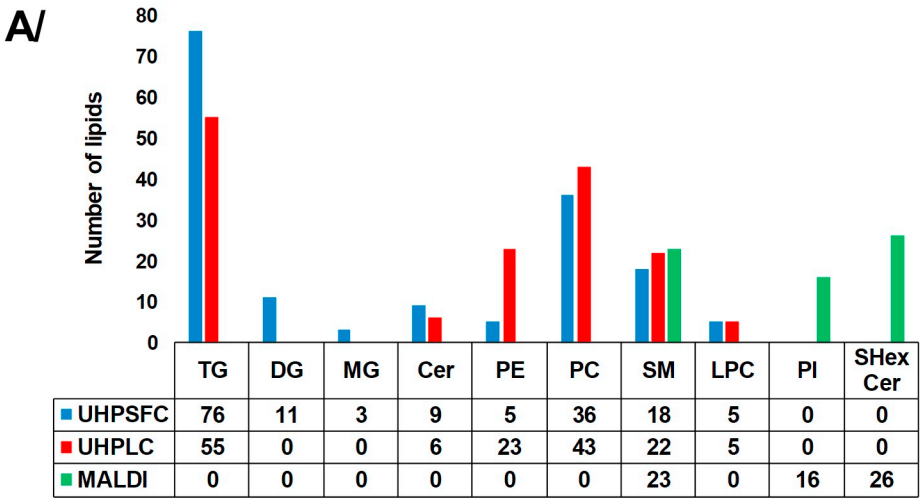

	TG	DG	MG	Cer	PE	PC	SM	LPC	PI	SHex Cer
UHPSFC	76	11	3	9	5	36	18	5	0	0
UHPLC	55	0	0	6	23	43	22	5	0	0
MALDI	0	0	0	0	0	0	23	0	16	26

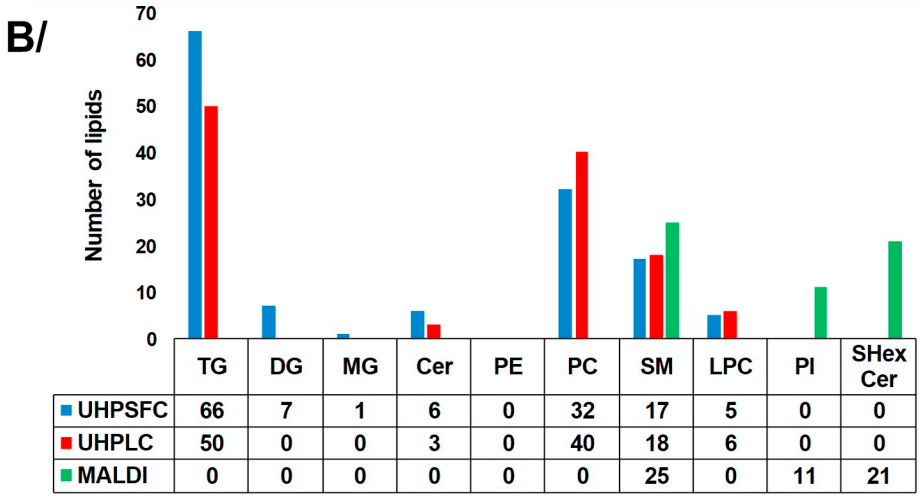

	TG	DG	MG	Cer	PE	PC	SM	LPC	PI	SHex Cer
UHPSFC	66	7	1	6	0	32	17	5	0	0
UHPLC	50	0	0	3	0	40	18	6	0	0
MALDI	0	0	0	0	0	0	25	0	11	21

Fig. 2. Number of quantified lipid species in A/ exosomes and B/ human plasma by UHPSFC/MS (blue), UHPLC/MS (red), and MALDI-MS (green).

2.2. Exosomes isolation

A commercial kit Invitrogen (Thermo Fisher Scientific) was used for the isolation of exosomes from human plasma. 600 µl was centrifuged to remove larger extracellular vesicles using 14,000 ×g at 4 °C for 35 min. 500 µl from bottom layer was transferred to a new centrifugation tube, 250 µl phosphate-buffered saline was added, and the mixture was thoroughly vortexed. 25 µl proteinase K was added, the sample was vortexed and incubated at 37 °C for 10 min. The mixture was mixed with 150 µl polyethylene glycol as a precipitation agent. The reaction mixture was incubated at 2–8 °C for 30 min. Exosomes were pelleted at the bottom of the tube by ultracentrifugation at 10,000 ×*g* at ambient temperature for 5 min. Pellets were washed and transferred to a new tube. The presence of exosomes was confirmed by the electron microscope and then stored at −80 °C prior to the analysis.

2.3. Lipid extraction

Pellets were dissolved in 120 µl methanol:water (1:1, v/v), and an aliquot of 100 µl of the exosomes suspensions or 25 µl of human plasma were used for total lipid extracts by a modified Folch lipid extraction [24]. Samples were spiked before the extraction with 17.5 µl of the IS Mix. The organic phase of the extract was evaporated under the stream of nitrogen and redissolved in 500 µl of mixture chloroform – 2-propanol (1:1, v/v). Total lipid extracts were stored at −80 °C and diluted 5 times with methanol – chloroform (1:1, v/v) mixture just before UHPSFC/MS and UHPLC/MS analyses. MALDI matrix 9-AA was dissolved in methanol – water mixture (4:1, v/v) to provide the concentration of 5 mg/mL and mixed with particular lipid extracts (1:1, v/v). The deposited amount of extract/matrix mixture was 1 µL, and the dried droplet crystallization was used for the sample deposition on the target plate. The pipetting of small aliquot of chloroform on MALDI plate spots before the application of extract/matrix mixture was applied to avoid the drop spreading.

2.4. UHPSFC conditions

UHPSFC experiments were performed on an Acquity UPC^2 instrument (Waters, Milford, MA, USA). A modified UHPSFC/MS method [25] for the lipidomic analysis was used with the following conditions: Viridis BEH column (100 mm × 3 mm, 1.7 µm, Waters), the flow rate 1.9 mL/min, the column temperature 60 °C, the injection volume 1 µL, the autosampler temperature 4 °C, the active back pressure regulator (ABPR) pressure 1,800 psi, and the gradient of methanol – water (99:1, v/v) mixture containing 30 mM of ammonium acetate as a modifier B: 0 min – 1% B, 1.5 min – 16% B, 7 min – 51% B, and 7.5 min – 1% B.

2.5. UHPLC conditions

A liquid chromatograph Agilent 1290 Infinity series (Agilent Technologies, Waldbronn, Germany) with the following conditions was used: Viridis BEH column (100 mm × 3 mm, 1.7 µm, Waters), the flow

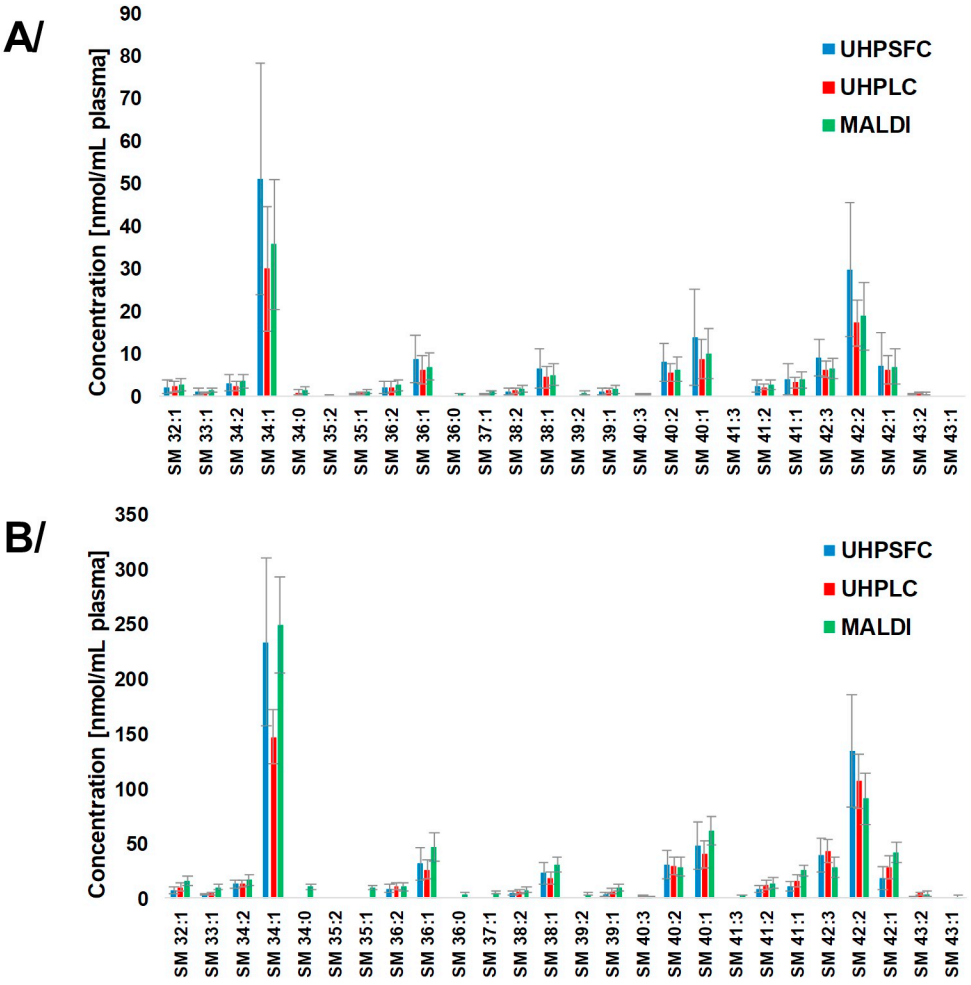

Fig. 3. Absolute molar concentration of sphingomyelins in A/ exosomes and B/ human plasma determined by UHPSFC/MS (blue), UHPLC/MS (red), and MALDI-MS (green).

Table 1
Ratios of molar lipid class absolute concentrations (plasma/exosomes).

Lipid class	UHPSFC	UHPLC	MALDI
Triacylglycerols	2.3	2.7	
Diacylglycerols	2.8		
Monoacylglycerols	0.6[a]		
Ceramides	2.3	2.9	
Phosphatidylcholines	6.6	7.0	
Sphingomyelins	3.4	5.5	6.1
Lysophosphatidylcholines	12.9	12.4	
Phosphatidylinositols			6.4
Sulfatides			6.7

[a] Only for one lipid species.

rate 0.5 mL/min, the injection volume 1 μL, the column temperature 40 °C, and the autosampler temperature 4 °C. The mobile phase gradient was set: 0 min – 100% A, 5 min – 84% A, and 10.5 min – 100% A, where phase A was 96% ACN + 4% H_2O 8 mM ammonium acetate and phase B was 98% H_2O + 2% ACN 8 mM ammonium acetate.

2.6. Mass spectrometry conditions

UHPSFC instrument was connected to the hybrid quadrupole – time of flight (QTOF) mass spectrometer Synapt G2-Si High Definition (Waters, Milford, MA, USA) by two T-pieces (Waters) enabling the backpressure control and mixing of column effluent with a make-up liquid. The mixture of methanol – water (99:1, v/v) containing 30 mM of ammonium acetate was used as the make-up liquid at the flow rate of 0.25 mL/min delivered by HPLC 515 pump (Waters). UHPLC/ESI-MS experiments were performed on Xevo G2-XS QTOF mass spectrometer (Waters, Milford, MA, USA). The sensitivity mode in positive-ion ESI was used with the following instrument parameters: the mass range *m/z* 50–1200, the capillary voltage 3.0 kV, the sampling cone 20 V, the source offset 90 V, the source temperature 150 °C, the drying temperature 500 °C, the cone gas flow 0.8 L/min, the drying gas flow 17 L/min, and the nebulizer gas pressure 4 bar. Leucine enkephalin was used as the lock mass for all experiments.

2.7. MALDI mass spectrometry conditions

Mass spectra were measured using high-resolution MALDI mass spectrometer LTQ Orbitrap XL (Thermo Fisher Scientific, Waltham, MA, USA) equipped with the nitrogen UV laser (337 nm, 60 Hz) with a beam diameter of about 80 μm × 100 μm. The LTQ Orbitrap instrument was operated in the negative-ion mode over a normal mass range *m/z* 400–2000 and the mass resolution was set to R = 100,000 (full width at half maximum (FWHM) definition, at *m/z* 400). The spiral outwards sample movement with 250 μm step size was used during the individual data acquisition. The laser energy corresponded to 2.7 μJ and 2 microscans/scan with 2 laser shots per micro scan at 36 different positions were accumulated for each measurement to achieve a reproducible signal. Each sample (matrix and body fluid extract mixture) was spotted five times. The total acquisition time of one sample including five consecutive spots was around 10 min.

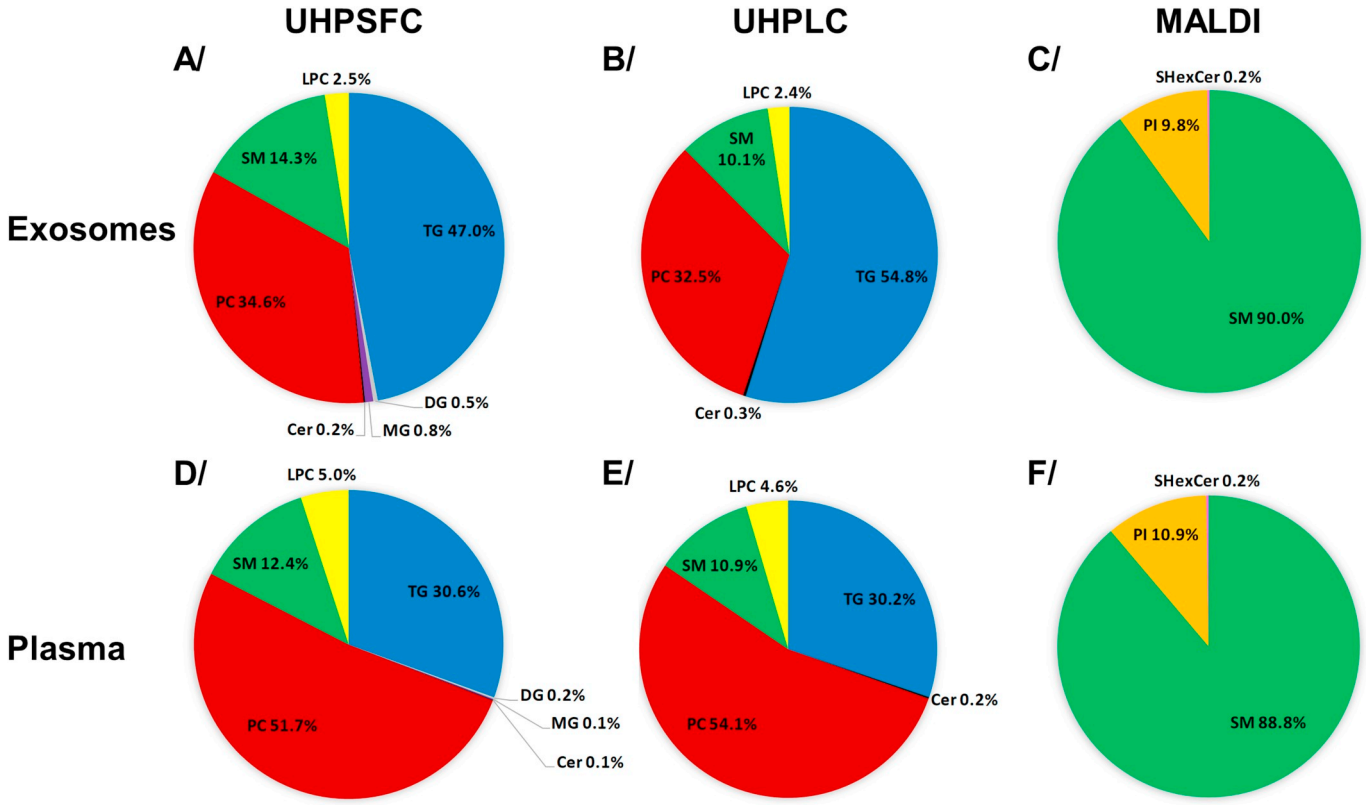

Fig. 4. Relative molar abundances for individual of lipid classes (TG, DG, MG, Cer, PC, PE, PI, SM, LPC, and SHexCer) in A-C/ exosomes and D-F/ human plasma. This comparison shows only lipids detected in both sample types. The concentrations of each class are related to the total concentration of lipids present in both type of material.

2.8. Data processing

UHPSFC/MS and UHPLC/MS data were measured in the continuum mode and then processed. The data were submitted for the noise reduction with the threshold of 20 by Waters Compression Tool, which caused data size reduction about 20–50 times. The lock mass correction was subsequently applied to obtain accurate masses, and data were finally converted to the centroid mode. MarkerLynx XS software was used to summarize *m/z* with the corresponding intensities for a given scan range depending on the lipid class, and afterwards data tables were exported as .txt files. The MS data were processed by a laboratory-made Excel macro script named LipidQuant with an embedded database [24]. Lipid species were detected according to accurate *m/z* values with the mass tolerance of 15 mDa. Each measurement was represented by one average MALDI-MS spectrum with thousands of *m/z* values.

The automatic peak assignment was subsequently performed, and particular *m/z* peaks were matched with deprotonated molecules from a database created during the identification procedure. This peak assignment resulted in the generation of the list of present *m/z* of studied lipids with the average intensities in particular spectra for each sample, which was used for further statistical evaluation. After the isotopic correction of signal responses, molar concentrations of the lipid species were calculated by relating the lipid species intensities to the intensity of the IS for the particular lipid class and the known concentration of the IS (Table S-2).

2.9. Statistical data analysis

Absolute and relative concentrations of lipid species were used for MDA by the SIMCA software, version 13.0.3 (Umetrics, Umeå, Sweden). The Pareto scaling and logarithm transformation were performed for the data normalization. Differences were investigated using statistical projection methods, e.g., PCA, OPLS-DA, and S-plot. Statistic parameters p-values, T-values, fold change, false discovery rate (FDR) were calculated for the evaluation of significant differences. Box plots were generated for most dysregulated lipid profiles in R free software. Sequences of samples were independently randomized for the isolation, extraction, and measurements to avoid possible bias during the statistical analysis.

2.10. Quality control

Pooled samples of exosome or plasma samples (representative mix of all samples) spiked with IS before the extraction were used for the quality control (QC) throughout the measurement. For monitoring of the instrumental performance and the sample preparation protocol, two types of quality control were applied. First, the measurement of the QC sample after every 24 samples reflecting the instrument performance and then the monitoring of each IS response in each sample during measurements, which allowed the assessment of the instrument performance or sample preparation error. The signal stability is represented by absolute intensities of QC samples for plasma by the Levey-Jennings graph (Fig. S-1), and the trends of other possibilities were equal.

3. Results

3.1. Identification of lipid species

Twelve apparently healthy men aged between 44 and 62 years with body mass index ranging from 20 to 30 were enrolled in this study (Table S-3). Initially, a nontargeted identification of lipids was performed separately for plasma and exosome samples using the pooled samples for these matrices. Individual lipids are identified based on retention times and accurate *m/z* measured by QTOF mass analyzer with high resolving power (ca. 20,000, FWHM) and high mass accuracy

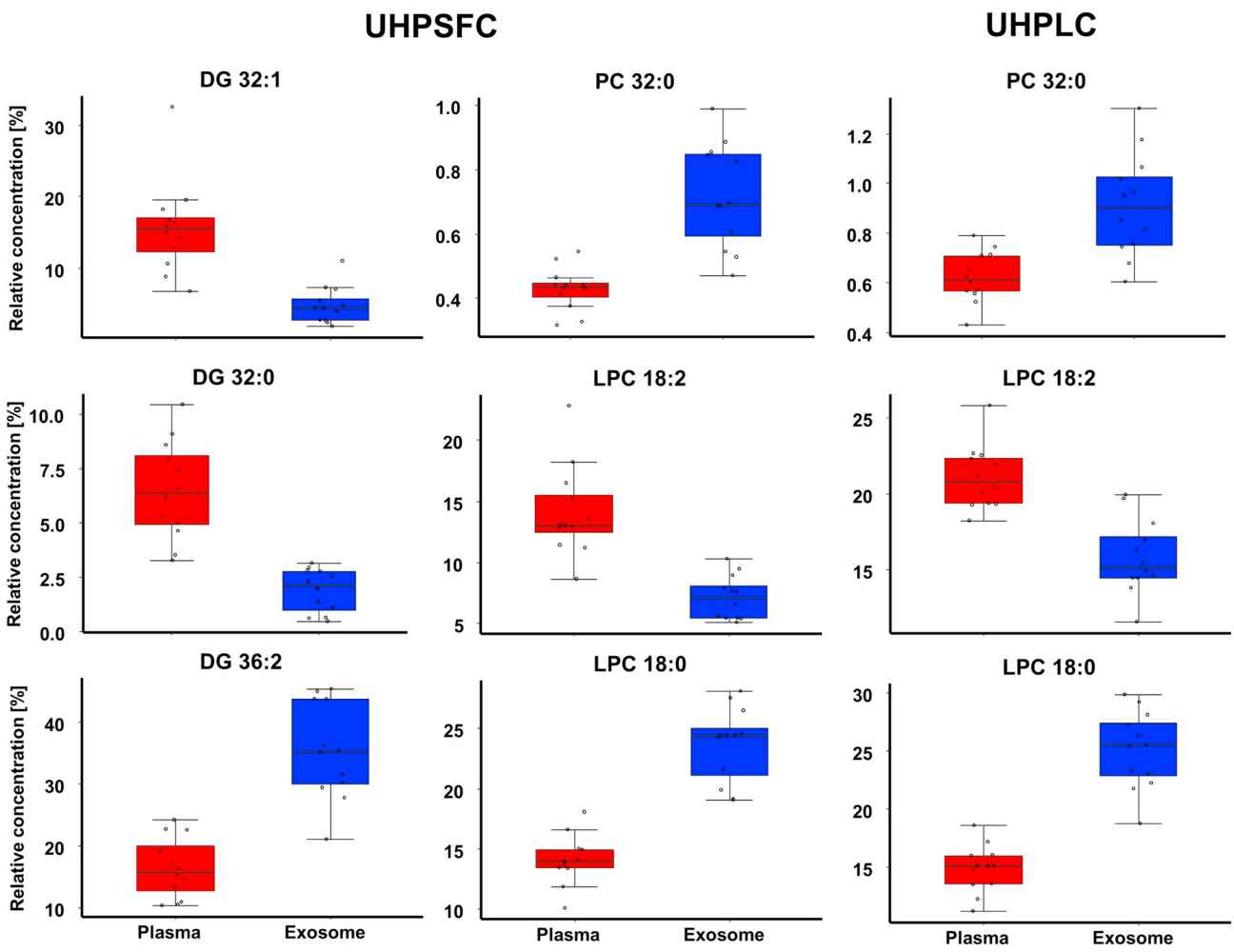

Fig. 5. Box plots for lipid species with the largest differences between exosomes and human plasma. Relative molar concentrations expressed in % lipid abundances within the class.

(< 5 ppm). MALDI-Orbitrap MS with the resolving power of about 100,000 (FWHM) and MS/MS spectra allows the identification of overlapping lipids. UHPSFC/MS and UHPLC/MS in hydrophilic interaction liquid chromatography mode enable the lipid class separation, where IS coelute together with lipid species from the same class in one chromatographic peak. The quantitative analysis is based on the comparison of the intensity of IS and intensities of individual lipid species. All methods were previously validated for the analysis of human body fluid samples [24,27].

3.2. Quantification of lipids

In total, we quantify 244 lipids in exosomes and 191 lipids in plasma by all MS techniques. UHPSFC/MS enables the determination of polar and nonpolar lipid classes, which resulted in the quantitation of highest number of lipid species (Fig. 2). UHPLC/MS is more sensitive for polar lipids, whereas nonpolar lipid classes (CE, MG, DG, TG, and Cer) coelute in the void volume of the system, which causes an overlap of adducts of DG and MG and hampering the quantification by this method. The quantitation of lipids in the void volume of the system for HILIC method can also lead to interferences of isobaric ions, which may cause discrepancies in the inter-method comparison of determined concentration. MALDI-MS with 9-aminoacridine as the matrix provides a selective ionization for anionic lipids in the negative-ion mode. Without any separation step, we observe overlaps of isobaric lipids [27], which enable the reliable quantification of only SM, PI, and SHexCer.

Cholesterol esters and free cholesterol (FC) are abundant molecules in human plasma, but their quantitation is complicated, as reported previously [29,30]. CE and FC typically undergo an excessive in-source fragmentation resulting in the formation of cholestadiene fragment ion at *m/z* 369.3516 (or 7D-cholestadiene fragment ion at *m/z* 376.3955 for labeled IS, respectively), which may disable their reliable quantitation on some mass spectrometric systems. It was reported [29] that the relation between cholestadiene and D7-cholestadiene is nonlinear, therefore this cannot be applied for the quantitation without the use of response factors. Höring et al. [30] demonstrated with FIA-HR-FTMS method that the resolving power of 140,000 at *m/z* 200 is necessary to resolve isobaric ions. We do not have a system with such resolving power, therefore we can only report identifications to avoid reporting non-reliable quantitative data for CE and FC.

The number of quantified lipids by individual MS methods is shown in Fig. 2, where the number of lipids in exosomes is higher in almost all cases. In particular, phosphatidylethanolamines are detected only in exosomes. The overlap of lipids present in exosomes and plasma are over 95% for all techniques. The summary is listed in Table S-4. More than 100 lipid species are determined for both UHPSFC/MS and UHPLC/MS independent of the biological material (Table S-5). Sphingomyelins are determined by all three methods, and the conformity is 18 SM for exosomes and 17 SM for plasma.

Although exosomes were isolated from human plasma, absolute molar concentrations of lipid species are expressed in nmol/mL of processed plasma, and average concentrations of all lipid species in exosomes, plasma, and references data [31,32] are shown in Table S-6. The comparison of concentrations within lipid classes is presented by bar

Table 2
The main up- and down-regulated lipid species based on relative concentration with the following statistical parameters: p-value, T-value, fold change, and false discovery rate (FDR).

Method	Regulation	Lipid	p-value	T-value	Fold change	FDR
UHPSFC	Down-regulated	DG 32:0	1.0E−05	−46.8	0.3	True
		TG 52:2	1.4E−05	−42.3	0.7	True
		LPC 18:2	2.5E−05	−42.6	0.5	True
		DG 32:1	9.8E−05	−38.6	0.3	True
		LPC 20:4	8.3E−04	−28.0	0.6	True
		Cer 34:1	1.6E−03	−26.9	0.7	True
	Up-regulated	LPC 18:0	3.2E−08	64.7	1.7	True
		DG 36:2	1.1E−06	51.5	2.2	True
		PC 32:0	4.5E−05	41.3	1.7	True
		DG 34:2	3.1E−04	31.4	1.5	True
		TG 49:2	4.0E−04	30.5	1.7	True
UHPLC	Down-regulated	LPC 18:2	1.3E−05	−40.8	0.8	True
		LPC 16:1	5.8E−05	−39.1	0.5	True
		LPC 18:1	1.7E−03	−27.3	0.7	True
		SM 42:3	4.4E−03	−23.2	0.8	True
		SM 40:3	4.6E−03	−22.9	0.8	True
		SM 42:2	1.4E−02	−19.3	0.9	True
		SM 43:2	2.4E−02	−17.6	0.8	True
	Up-regulated	LPC 18:0	3.7E−08	65.5	1.7	True
		PC 32:0	5.5E−04	31.1	1.5	True
		SM 38:1	5.8E−03	22.1	1.2	True
		PC 35:1	1.4E−02	19.4	1.3	True
		PC 30:0	1.8E−02	19.1	2.0	True
		SM 36:1	2.3E−02	17.6	1.2	True
		PC 36:1	3.1E−02	17.3	1.4	True
MALDI	Down-regulated	SM 35:1	7.3E−06	−42.3	0.7	True
		SM 34:1	5.9E−04	−29.0	0.9	True
		SM 34:0	1.2E−02	−20.6	0.8	True
	Up-regulated	PI 40:5	4.4E−06	44.2	2.1	False
		SM 40:2	6.2E−05	37.4	1.3	True
		SM 42:3	3.0E−04	31.2	1.4	True
		PI 40:6	9.7E−04	28.2	2.7	False
		SM 42:2	1.2E−03	28.0	1.2	True

graphs (Fig. S-2) for exosomes and plasma using three different methods (UHPSFC/MS, UHPLC/MS, and MALDI-MS). Corresponding concentrations of TG, Cer, PC, PE, and LPC are determined in both materials by UHPSFC/MS and UHPLC/MS. The comparability of all three methods is illustrated for SM (Fig. 3). In most cases, differences among methods are acceptable, as illustrated by the correlation analysis (Fig. S-3), but there are also some cases, where discrepancies cannot be classified as negligible, for example TG 48:1, Cer 42:1, Cer 42:2, and SM 34:1. The reason of these differences is multifactorial, and it is not so easy to overcome these problems, as reported in previous works [24,28].

Our results are compared with literature data [31,32] (Fig. S-2), which used NIST plasma for interlaboratory comparison. Differences are mostly of minor extend and can be partially attributed to the fact that the analyzed plasma is not identical. The largest differences are noticed for DG 34:0, DG 36:4, DG 36:3, PC 34:2, PC 34:1, SM 34:1, and PI 38:4. Some lipids classes are reported only in our work (e.g., MG and SHexCer), other classes are missing in comparison to mentioned papers, such as PE.

Ratios of average absolute concentrations in plasma and exosomes are summarized in Table 1 to illustrate that average concentrations in plasma are approximately five times higher than those in exosomes. This comparison shows only lipids detected in both sample types. For graphic visualization of class concentration changes, pie charts (Fig. 4) are used, where the biggest changes correspond to TG, DG, PC and LPC unlike to SM, PI, and sulfatides that show similar profiles in both biological matrices.

3.3. Statistical analysis

The transformation of molar concentration of exosomes and plasma to the relative concentration (% of lipid molar concentration within the class) provides a complementary view with better visualization of changes inside individual lipid classes. The score plot of unsupervised PCA method (Fig. S-4A) shows a good clustering of exosomes and plasma (Q2 = 0.876). The model based on relative concentrations (Fig. S-4B) also demonstrates a relatively good clustering (Q2 = 0.614) for UHPSFC/MS. UHPLC/MS and MALDI-MS models show the same trends, but the quality of statistical models is slightly worse in comparison to models based on UHPSFC/MS. The clustering of QC almost in one point illustrates the quality of data set. The prediction of supervised OPLS-DA methods based on relative concentrations is for UHPSFC/MS (Q2 = 0.935), for UHPLC/MS (Q2 = 0.761), and for MALDI-MS (Q2 = 0.769). S-plots (Fig. S-5) are generated from OPLS-DA and identify the most pronounced differences between both sample groups, where the upper right part of the S-plot indicates the most up-regulated lipids in exosomes, and the lower left part corresponds to the most down-regulated lipids in exosomes. Lipids in the center part of S-plot have low statistical significance, therefore they are not annotated. The lipid classes with most pronounce differences include DG, PC, and LPC, whereby unsaturated LPC (16:1, 18:2, 18:1, and 20:4) and shorter DG (32:1 and 32:0) are down-regulated, and saturated LPC (18:0), longer DG (34:2 and 36:2), and PC (30:0, 32:0, 35:1, and 36:1) are up-regulated in exosomes. Relative data for individual techniques are calculated from different numbers of quantified lipids, which may cause slight shifts in S-plots with most up- and down-regulated lipids, but the main trends are identical, as illustrated on box plots shown in Fig. 5 for lipid species with the largest differences between exosomes and plasma.

Furthermore, other statistical parameters may illustrate the extent of differences between biological materials through various MS methods (Table 2). P-values are calculated using *t*-test, and all values lower than 0.05 are reported as statistically significant. Lipids are sorted by the lowest value. Critical values are evaluated by Benjamini-Hochberg procedure with a false discovery rate of 25%. Lipids PI 40:6 and PI 40:5 are excluded based on this test. The fold change is a ratio of average concentrations of lipid species in exosomes divided by average concentrations in plasma. Values lower than 0.5 and higher than 1.5 indicate significant differences.

4. Discussion

The lipid composition of total exosomes isolated from human plasma was analyzed in 12 healthy volunteers. The exosomal lipidome contains more measurable lipid species in comparison to plasma (Fig. 2). This is in agreement with the fact that exosomes are large vesicles consisting of lipid rich double-layer membrane in comparison to plasma being an aqueous biological fluid. Both absolute molar concentrations (nmol/mL plasma) and relative concentrations (%) for individual lipid classes are reported here, because it provides the complementary approach of visualization of the results. Absolute molar concentrations are related to the volume of processed plasma, therefore molar concentrations in plasma are approximately 5 times higher, because plasma has other sources of lipids in addition to exosomes, which increases the overall molar concentrations in plasma. Relative concentrations clearly illustrate the enrichment of specific lipids within one class over other lipid species from the same class.

Analyzed lipids represent several important lipid classes within three lipid categories of glycerolipids, glycerophospholipids, and sphingolipids. In the following discussion, we differentiate lipid classes known as membrane lipids (PC, LPC, Cer, and SM) from lipids occurring in the internal space of lipid membrane, but not participating on the membrane structure (TG, DG, and MG). We are aware that such strict differentiation is slightly oversimplified, because DG may also play a role as the membrane anchor for protein-kinase D1 [33], nevertheless this helps to visualize some important trends described here. The principal finding is a significant relative increase of TG in exosomes in comparison to plasma (Fig. 4). We hypothesize that TG transfer from lipoproteins to exosomes occurs after the release into the blood stream,

where lipoproteins could adhere and fuse with exosomes. A similar phenomenon of lipoprotein-exosomal fusion was described earlier for pure LDL and exosomal fractions, as evaluated by electron microscopy [34]. The reason for exosomal uptake and transport of TG is unknown so far, but it may be important to maintain the basal TG metabolism independent from lipoproteins. The role of exosomes as a source of substrates and enzymes for distant metabolic sites has been proposed [35]. A possible role of exosomes in the lipid accumulation and transport was also described for cholesterol in atherosclerosis [36]. The transport of lipids (mainly TG) via adipose tissue derived exosomes was recently described in mice [37], but present data suggest indirectly for the first time the similar phenomenon with the possible role of TG rich intra-exosomal environment in humans, which may have also important clinical consequences.

The second highly enriched lipid class in exosomes was DG, which may be the product of intra-exosomal metabolism of TG via lipases degradation or produced from PC via action of phospholipases known for exosomes. Many different lipid metabolizing enzymes are transported to exosomes to process their lipids content [38]. DG are possibly on the crossroad of exosomal membrane and the internal lipid metabolism, where membrane PC are a substrate for the metabolic conversion to DG, PA, LPC and the further conversion to LPA and secondly the conversion of intra-exosomal TG to DG followed by the release of fatty acids. Exosomes were recently described as vesicles, which deliver fatty acids to specific tissues or cells [39], and the source of fatty acids may be TG rich intra-exosomal space and lipase activity. The conversion of TG to DG is indirectly supported by Fig. S-6 with the relations of TG, DG and MG in plasma and exosomes.

It is important to point out that exosomal biogenesis has an impact on the constitution of the lipidomic membrane. The biogenesis of exosomes is associated with the endosomal pathway starting from endocytosis and followed to early- and late-endosomes, therefore the membrane composition reflects the endosome membrane rather than plasmatic lipids [1,40]. The second important fact is that exosomes represent small compact spheroid object with the resistant membrane, which prolongs their half-life in plasma, e.g., in comparison to microvesicles, which are derived by direct budding from plasma membrane [2]. This explains different lipid composition with the lower amount of PC and LPC and the increased amount of SM and Cer (Fig. S-6). This picture is similar to previously described lipid alterations in the exosomal membrane [40,41], e.g., in exosomes from dendritic cells [42]. It should be emphasized that increased amounts of lipids with fully saturated fatty acids in their structures are detected in exosomes, such as LPC 18:0 and PC 32:0 and decreased unsaturated species, e.g., LPC 18:2. This molecular pattern in the membrane helps to keep the rigid durable structure [2,40,41]. A decrease in LPC 18:2 may also indicate the activity of PLD, which has been described in exosomes and producing LPA [35,40].

PE were determined only in exosomes, because the concentrations in plasma were below LOQ. It is important to point out that PE have also to be present in plasma, because plasma is the source of exosomes, but this finding should be interpreted as the relative increase of PE in exosomes. PE are known to participate in the generation of lipid droplets and membranous structures. Together with a lower level of PC, it suggests membranous structures of exosomes, which is in concordance with the nature of exosomes [43].

Profiles of SM as the major sphingolipid class were the same in plasma and exosomes without statistically relevant changes in agreement with the literature [40]. This indicates that SM play some membrane housekeeping role, and therefore the profiles have to be maintained in relatively common pattern.

5. Conclusions

Exosomes isolated from human plasma of 12 healthy volunteers were analyzed by 3 different MS techniques, and the lipidomic composition was compared with their plasma to highlight differences. Absolute molar concentrations of lipid species from 10 lipid classes were determined, and results were compared among all methods and also with previously published data for human plasma. The expression of relative concentrations for individual lipid classes was used for the visualization of changes inside classes with the largest differences, such as TG, DG, PC, and LPC. Various statistical tools were applied for the visualization of major differences. A significant enrichment of TG in exosomes was detected, which may be explained by the fusion of exosomes with TG rich lipoprotein particles. The TG rich intra-exosomal environment was previously described in mice with the possible pathophysiological role, but we have indirectly observed here a similar situation in human plasma derived exosomes. The significance of this phenomenon is possibly in the maintenance of the basal TG metabolism independent of lipoproteins. Other lipids in exosomal membrane confirm that the origin is different from plasma membrane. The molecular pattern with increased amounts of lipids with saturated fatty acids supports the idea of small highly rigid membranous particles with prolonged half-life in the bloodstream.

Our results show main differences between exosomes isolated from human plasma and plasma. Exosomes are still underexplored nanoparticles, and future improvements in the isolation of exosomes including particular exosome fractions, can result in a better understanding of cell-to-cell communication and other roles of exosomes at the cellular level, which may have a potential for early detection of serious disorders.

Supplementary data to this article can be found online at https://doi.org/10.1016/j.bbalip.2020.158634.

Declaration of competing interest

The authors declare that they have no known competing financial interests or personal relationships that could have appeared to influence the work reported in this paper.

Acknowledgments

This work was supported by Czech Science Foundation (GAČR) project No. 18-12204S. L.K. acknowledges the support of institutional program of the Charles University in Prague (UNCE 204064). Authors would like to acknowledge Eva Cífková for the development of LipidQuant Excel macro script for processing of lipidomic data.

References

[1] C. Bissig, J. Gruenberg, Lipid sorting and multivesicular endosome biogenesis, CSH Perspect. Biol. 5 (2013) a016816, https://doi.org/10.1101/cshperspect.a016816.
[2] M. Record, S. Silvente-Poirot, M. Poirot, M.J.O. Wakelam, Extracellular vesicles: lipids as key components of their biogenesis and functions, J. Lipid Res. 59 (2018) 1316–1324, https://doi.org/10.1194/jlr.E086173.
[3] Y. Zhang, Y. Liu, H. Liu, W.H. Tang, Exosomes: biogenesis, biologic function and clinical potential, Cell Biosci. 9 (2019) 19, https://doi.org/10.1186/s13578-019-0282-2.
[4] M. Verma, T.K. Lam, E. Hebert, R.L. Divi, Extracellular vesicles: potential applications in cancer diagnosis, prognosis, and epidemiology, BMC Clin. Pathol. 15 (2015) 6, https://doi.org/10.1186/s12907-015-0005-5.
[5] A. Llorente, T. Skotland, T. Sylvänne, D. Kauhanen, T. Róg, A. Orłowski, I. Vattulainen, K. Ekroos, K. Sandvig, Molecular lipidomics of exosomes released by PC-3 prostate cancer cells, BBA-Mol. Cell Biol. L. 1831 (2013) 1302–1309, https://doi.org/10.1016/j.bbalip.2013.04.011.
[6] T. Skotland, K. Ekroos, D. Kauhanen, H. Simolin, T. Seierstad, V. Berge, K. Sandvig, A. Llorente, Molecular lipid species in urinary exosomes as potential prostate cancer biomarkers, Eur. J. Cancer 70 (2017) 122–132, https://doi.org/10.1016/j.ejca.2016.10.011.
[7] T.A. Lydic, S. Townsend, C.G. Adda, C. Collins, S. Mathivanan, G.E. Reid, Rapid and comprehensive 'shotgun' lipidome profiling of colorectal cancer cell derived exosomes, Methods 87 (2015) 83–95, https://doi.org/10.1016/j.ymeth.2015.04.014.
[8] T.W.M. Fan, X. Zhang, C. Wang, Y. Yang, W.-Y. Kang, S. Arnold, R.M. Higashi, J. Liu, A.N. Lane, Exosomal lipids for classifying early and late stage non-small cell lung cancer, Anal. Chim. Acta 1037 (2018) 256–264, https://doi.org/10.1016/j.aca.2018.02.051.
[9] X. Chen, H. Chen, M. Dai, J. Ai, Y. Li, B. Mahon, S. Dai, Y. Deng, Plasma lipidomics

profiling identified lipid biomarkers in distinguishing early-stage breast cancer from benign lesions, Oncotarget 7 (2016) 36622–36631, https://doi.org/10.18632/oncotarget.9124.
[10] G. Pocsfalvi, C. Stanly, I. Fiume, K. Vékey, Chromatography and its hyphenation to mass spectrometry for extracellular vesicle analysis, J. Chromatogr. A 1439 (2016) 26–41, https://doi.org/10.1016/j.chroma.2016.01.017.
[11] M.P. Zaborowski, L. Balaj, X.O. Breakefield, C.P. Lai, Extracellular vesicles: composition, biological relevance, and methods of study, BioScience 65 (2015) 783–797, https://doi.org/10.1093/biosci/biv084.
[12] J.S. Yang, J.C. Lee, S.K. Byeon, K.H. Rha, M.H. Moon, Size dependent lipidomic analysis of urinary exosomes from patients with prostate cancer by flow field-flow fractionation and nanoflow liquid chromatography-tandem mass spectrometry, Anal. Chem. 89 (2017) 2488–2496, https://doi.org/10.1021/acs.analchem.6b04634.
[13] A. de Menezes-Neto, M.J.F. Sáez, I. Lozano-Ramos, J. Segui-Barber, L. Martin-Jaular, J.M.E. Ullate, C. Fernandez-Becerra, F.E. Borrás, H.A. del Portillo, Size-exclusion chromatography as a stand-alone methodology identifies novel markers in mass spectrometry analyses of plasma-derived vesicles from healthy individuals, J Extracell Vesicles 4 (2015) 27378, https://doi.org/10.3402/jev.v4.27378.
[14] L.A. Aqrawi, H.K. Galtung, B. Vestad, R. Øvstebø, B. Thiede, S. Rusthen, A. Young, E.M. Guerreiro, T.P. Utheim, X. Chen, Ø. Utheim, Ø. Palm, J.L. Jensen, Identification of potential saliva and tear biomarkers in primary Sjögren's syndrome, utilising the extraction of extracellular vesicles and proteomics analysis, Arthritis Res. Ther. 19 (2017) 14, https://doi.org/10.1186/s13075-017-1228-x.
[15] H. Roberg-Larsen, K. Lund, K.E. Seterdal, S. Solheim, T. Vehus, N. Solberg, S. Krauss, E. Lundanes, S.R. Wilson, Mass spectrometric detection of 27-hydroxycholesterol in breast cancer exosomes, J. Steroid Biochem. Mol. Biol. 169 (2017) 22–28, https://doi.org/10.1016/j.jsbmb.2016.02.006.
[16] B.-Y. Chen, C.W.-H. Sung, C. Chen, C.-M. Cheng, D.P.-C. Lin, C.-T. Huang, M.-Y. Hsu, Advances in exosomes technology, Clin. Chim. Acta 493 (2019) 14–19, https://doi.org/10.1016/j.cca.2019.02.021.
[17] C. Admyre, S.M. Johansson, K.R. Qazi, J.-J. Filén, R. Lahesmaa, M. Norman, E.P.A. Neve, A. Scheynius, S. Gabrielsson, Exosomes with immune modulatory features are present in human breast milk, J. Immunol. 179 (2007) 1969, https://doi.org/10.4049/jimmunol.179.3.1969.
[18] G. Pocsfalvi, C. Stanly, A. Vilasi, I. Fiume, G. Capasso, L. Turiák, E.I. Buzas, K. Vékey, Mass spectrometry of extracellular vesicles, Mass Spectrom. Rev. 35 (2016) 3–21, https://doi.org/10.1002/mas.21457.
[19] M. Holčapek, G. Liebisch, K. Ekroos, Lipidomic analysis, Anal. Chem. 90 (2018) 4249–4257, https://doi.org/10.1021/acs.analchem.7b05395.
[20] M.R. Wenk, The emerging field of lipidomics, Nat. Rev. Drug Discov. 4 (2005) 594–610, https://doi.org/10.1038/nrd1776.
[21] R.B. Chan, T.G. Oliveira, E.P. Cortes, L.S. Honig, K.E. Duff, S.A. Small, M.R. Wenk, G. Shui, G. Di Paolo, Comparative lipidomic analysis of mouse and human brain with Alzheimer disease, J. Biol. Chem. 287 (2012) 2678–2688, https://doi.org/10.1074/jbc.M111.274142.
[22] Z. Wang, E. Klipfell, B.J. Bennett, R. Koeth, B.S. Levison, B. DuGar, A.E. Feldstein, E.B. Britt, X. Fu, Y.-M. Chung, Y. Wu, P. Schauer, J.D. Smith, H. Allayee, W.H.W. Tang, J.A. DiDonato, A.J. Lusis, S.L. Hazen, Gut flora metabolism of phosphatidylcholine promotes cardiovascular disease, Nature 472 (2011) 57–63, https://doi.org/10.1038/nature09922.
[23] E. Fahy, S. Subramaniam, R.C. Murphy, M. Nishijima, C.R.H. Raetz, T. Shimizu, F. Spener, G. van Meer, M.J.O. Wakelam, E.A. Dennis, Update of the LIPID MAPS comprehensive classification system for lipids, J. Lipid Res. 50 (2009) S9–S14, https://doi.org/10.1194/jlr.R800095-JLR200.
[24] M. Lísa, E. Cífková, M. Khalikova, M. Ovčačíková, M. Holčapek, Lipidomic analysis of biological samples: comparison of liquid chromatography, supercritical fluid chromatography and direct infusion mass spectrometry methods, J. Chromatogr. A 1525 (2017) 96–108, https://doi.org/10.1016/j.chroma.2017.10.022.
[25] M. Lísa, M. Holčapek, High-throughput and comprehensive lipidomic analysis using ultrahigh-performance supercritical fluid chromatography–mass spectrometry, Anal. Chem. 87 (2015) 7187–7195, https://doi.org/10.1021/acs.analchem.5b01054.
[26] D. Wolrab, R. Jirásko, M. Chocholoušková, O. Peterka, M. Holčapek, Oncolipidomics: mass spectrometric quantitation of lipids in cancer research, TrAC Trends Anal Chem (2019), https://doi.org/10.1016/j.trac.2019.04.012.
[27] R. Jirásko, M. Holčapek, M. Khalikova, D. Vrána, V. Študent, Z. Prouzová, B. Melichar, MALDI orbitrap mass spectrometry profiling of dysregulated sulfoglycosphingolipids in renal cell carcinoma tissues, J. Am. Soc. Mass Spectrom. 28 (2017) 1562–1574, https://doi.org/10.1007/s13361-017-1644-9.
[28] D. Wolrab, M. Chocholoušková, R. Jirásko, O. Peterka, M. Holčapek, Validation of lipidomic analysis by supercritical fluid chromatography- and hydrophilic interaction liquid chromatography- mass spectrometry, Anal Bioanal Chem (2020) (accepted).
[29] S. Gallego, K. Hojlund, C. Ejsing, Easy, fast, and reproducible quantification of cholesterol and other lipids in human plasma by combined high resolution MSX and FTMS analysis, J. Am. Soc. Mass Spectrom. 29 (2018) 34–41, https://doi.org/10.1007/s13361-017-1829-2.
[30] M. Höring, C.S. Ejsing, M. Hermansson, G. Liebisch, Quantification of cholesterol and cholesteryl ester by direct flow injection high-resolution Fourier transform mass spectrometry utilizing species-specific response factors, Anal. Chem. 91 (2019) 3459–3466, https://doi.org/10.1021/acs.analchem.8b05013.
[31] J.A. Bowden, A. Heckert, C.Z. Ulmer, C.M. Jones, J.P. Koelmel, L. Abdullah, L. Ahonen, Y. Alnouti, A.M. Armando, J.M. Asara, T. Bamba, J.R. Barr, J. Bergquist, C.H. Borchers, J. Brandsma, S.B. Breitkopf, T. Cajka, A. Cazenave-Gassiot, A. Checa, M.A. Cinel, R.A. Colas, S. Cremers, E.A. Dennis, J.E. Evans, A. Fauland, O. Fiehn, M.S. Gardner, T.J. Garrett, K.H. Gotlinger, J. Han, Y.Y. Huang, A.H.P. Neo, T. Hyotylainen, Y. Izumi, H.F. Jiang, H.L. Jiang, J. Jiang, M. Kachman, R. Kiyonami, K. Klavins, C. Klose, H.C. Kofeler, J. Kolmert, T. Koal, G. Koster, Z. Kuklenyik, I.J. Kurland, M. Leadley, K. Lin, K.R. Maddipati, D. McDougall, P.J. Meikle, N.A. Mellett, C. Monnin, M.A. Moseley, R. Nandakumar, M. Oresic, R. Patterson, D. Peake, J.S. Pierce, M. Post, A.D. Postle, R. Pugh, Y.P. Qiu, O. Quehenberger, P. Ramrup, J. Rees, B. Rembiesa, D. Reynaud, M.R. Roth, S. Sales, K. Schuhmann, M.L. Schwartzman, C.N. Serhan, A. Shevchenko, S.E. Somerville, L.S. John-Williams, M.A. Surma, H. Takeda, R. Thakare, J.W. Thompson, F. Torta, A. Triebl, M. Trotzmuller, S.J.K. Ubhayasekera, D. Vuckovic, J.M. Weir, R. Welti, M.R. Wenk, C.E. Wheelock, L.B. Yao, M. Yuan, X.Q.H. Zhao, S.L. Zhou, Harmonizing lipidomics: NIST interlaboratory comparison exercise for lipidomics using SRM 1950-Metabolites in Frozen Human Plasma, J Lipid Res 58 (2017) 2275–2288, https://doi.org/10.1194/jlr.M079012.
[32] O. Quehenberger, A.M. Armando, A.H. Brown, S.B. Milne, D.S. Myers, A.H. Merrill, S. Bandyopadhyay, K.N. Jones, S. Kelly, R.L. Shaner, C.M. Sullards, E. Wang, R.C. Murphy, R.M. Barkley, T.J. Leiker, C.R.H. Raetz, Z.Q. Guan, G.M. Laird, D.A. Six, D.W. Russell, J.G. McDonald, S. Subramaniam, E. Fahy, E.A. Dennis, Lipidomics reveals a remarkable diversity of lipids in human plasma, J. Lipid Res. 51 (2010) 3299–3305, https://doi.org/10.1194/jlr.M009449.
[33] C.F. Cowell, H. Döppler, I.K. Yan, A. Hausser, Y. Umezawa, P. Storz, Mitochondrial diacylglycerol initiates protein-kinase-D1-mediated ROS signaling, J. Cell Sci. 122 (2009) 919–928, https://doi.org/10.1242/jcs.041061.
[34] B.W. Sódar, Á. Kittel, K. Pálóczi, K.V. Vukman, X. Osteikoetxea, K. Szabó-Taylor, A. Németh, B. Sperlágh, T. Baranyai, Z. Giricz, Z. Wiener, L. Turiák, L. Drahos, É. Pállinger, K. Vékey, P. Ferdinandy, A. Falus, E.I. Buzás, Low-density lipoprotein mimics blood plasma-derived exosomes and microvesicles during isolation and detection, Sci. Rep. 6 (2016) 24316, https://doi.org/10.1038/srep24316.
[35] C. Subra, D. Grand, K. Laulagnier, A. Stella, G. Lambeau, M. Paillasse, P. De Medina, B. Monsarrat, B. Perret, S. Silvente-Poirot, M. Poirot, M. Record, Exosomes account for vesicle-mediated transcellular transport of activatable phospholipases and prostaglandins, J. Lipid Res. 51 (2010) 2105–2120, https://doi.org/10.1194/jlr.M003657.
[36] L. Zakharova, M. Svetlova, A.F. Fomina, T cell exosomes induce cholesterol accumulation in human monocytes via phosphatidylserine receptor, J. Cell. Physiol. 212 (2007) 174–181, https://doi.org/10.1002/jcp.21013.
[37] S.E. Flaherty, A. Grijalva, X. Xu, E. Ables, A. Nomani, A.W. Ferrante, A lipase-independent pathway of lipid release and immune modulation by adipocytes, Science 363 (2019) 989–993, https://doi.org/10.1126/science.aaw2586.
[38] K. Sagini, E. Costanzi, C. Emiliani, S. Buratta, L. Urbanelli, Extracellular vesicles as conveyors of membrane-derived bioactive lipids in immune system, Int. J. Mol. Sci. 19 (2018) 1227, https://doi.org/10.3390/ijms19041227.
[39] N.A. Garcia, H. González-King, E. Grueso, R. Sánchez, A. Martinez-Romero, B. Jávega, J.E. O'Connor, P.J. Simons, A. Handberg, P. Sepúlveda, Circulating exosomes deliver free fatty acids from the bloodstream to cardiac cells: possible role of CD36, PLoS One 14 (2019) e0217546, , https://doi.org/10.1371/journal.pone.0217546.
[40] T. Skotland, K. Sandvig, A. Llorente, Lipids in exosomes: current knowledge and the way forward, Prog. Lipid Res. 66 (2017) 30–41, https://doi.org/10.1016/j.plipres.2017.03.001.
[41] C. Subra, K. Laulagnier, B. Perret, M. Record, Exosome lipidomics unravels lipid sorting at the level of multivesicular bodies, Biochimie 89 (2007) 205–212, https://doi.org/10.1016/j.biochi.2006.10.014.
[42] K. Laulagnier, C. Motta, S. Hamdi, S. Roy, F. Fauvelle, J.-F. Pageaux, T. Kobayashi, J.-P. Salles, B. Perret, C. Bonnerot, M. Record, Mast cell- and dendritic cell-derived exosomes display a specific lipid composition and an unusual membrane organization, Biochem. J. 380 (2004) 161–171, https://doi.org/10.1042/bj20031594.
[43] J.N. van der Veen, J.P. Kennelly, S. Wan, J.E. Vance, D.E. Vance, R.L. Jacobs, The critical role of phosphatidylcholine and phosphatidylethanolamine metabolism in health and disease, BBA-Biomembranes (2017) (1859) 1558–1572, https://doi.org/10.1016/j.bbamem.2017.04.006.